Chemistry of Inorganic Materials 3 (2024) 100049

Contents lists available at ScienceDirect

Chemistry of Inorganic Materials

journal homepage: www.elsevier.com/locate/cinorg

A novel Pt^{2+} complex containing 1,4-benzodioxan-6-amine: Stability, DNA binding, and antitumor effects against human breast cancer cells

Meiry L. Lacerda [a], Carla D. Lopes [b,c], Raphael T.C. Silva [a], Renan D. Zanetti [d], Mariete B. Moreira [d,e], Adelino V.G. Netto [d], Wesley A. Souza [a,f], Sérgio de Albuquerque [c], Drielly A. Paixão [a,**], Wendell Guerra [a,*]

[a] Instituto de Química, Universidade Federal de Uberlândia, Campus Santa Monica, Uberlândia, MG, Brazil
[b] Centro Universitário Estácio de Ribeirão Preto, Ribeirão Preto, SP, Brazil
[c] Departamento de Análises Clínicas, Toxicológicas e Bromatológicas, Faculdade de Ciências Farmacêuticas de Ribeirão Preto, Universidade de São Paulo, Ribeirão Preto, SP, Brazil
[d] Instituto de Química, Universidade Estadual Paulista, Araraquara, SP, Brazil
[e] Departamento de Química, Universidade Estadual de Londrina, Londrina, PR, Brazil
[f] Instituto de Ciências Exatas e da Terra, Campus Universitário Do Araguaia, Universidade Federal Do Mato Grosso, Pontal Do Araguaia, MT, Brazil

ARTICLE INFO

Keywords:
Platinum(II) complexes
Amines
Solvolysis
Anticancer activity
DNA
Fluorescence spectroscopy

ABSTRACT

In this work, a new platinum(II) complex was prepared by the reaction of K_2PtCl_4 with 1,4-benzodioxan-6-amine (bda) at room temperature in the molar ratio 2:1 (L:M). The complex was characterized by physicochemical (elemental analysis, TGA/DTA, and conductivity measurements) and spectroscopic methods (UV–Vis, FTIR, ^{1}H, ^{13}C and ^{195}Pt NMR). According to the spectroscopic data, two bda ligands coordinate to the platinum ion in a monodentate manner through the nitrogen atom to give the complex *cis*-$[PtCl_2(bda)_2]$. Stability studies were carried out under different conditions and showed that the complex is stable in pure DMF, although it undergoes slow solvolysis in DMSO. The interaction of this complex with calf thymus DNA (CT-DNA) was studied using circular dichroism (CD), electronic absorption and fluorescence spectroscopy. The complex binds to CT-DNA with a K_b value of 1.06×10^3 M^{-1} and according to data from CD and fluorescence spectroscopy, appears to interact with DNA by electrostatic forces and or other no intercalative binding mode. Compared to cisplatin, the complex exhibited good cytotoxic activity and selectivity against the MCF-7 tumor cell line, displaying an IC_{50} value of 17.33 ± 1.1 μM, as well as inhibited MCF-7 cells migration.

1. Introduction

The discovery of the antitumor activity of cisplatin is a milestone in the chemotherapy of cancer, since this metal-based drug exhibited a remarkable therapeutic efficacy for various types of solid tumors and outstanding activity against metastatic testicular germ-cell cancer achieving a high cure rate [1,2]. Although cisplatin is highly effective against several types of human cancer, this complex present an acquired or intrinsic resistance and severe side effects that reduce its effectiveness [3–6]. In an attempt to overcome these drawbacks, the synthesis of more effective and safer compounds is highly desirable for the development of new anticancer drugs. In this sense, the drugs carboplatin and oxaliplatin were later developed and released for clinical use. However, they also have severe side effects and resistance, although when compared to cisplatin, both are less nephrotoxic [7–10].

Despite the advances in anticancer drug development, the serious side effects, the tumor cell resistance against clinically used platinum drugs and the high mortality rates involving various types of cancer stimulate the search for new platinum complexes. In this sense, complexes of the type $[PtCl_2(L)_2]$ (L = *N*-donor ligands) are very interesting in terms of their anticancer potentials and arouse great interest. An example is the *cis*-ammine-dichlorido-2-methylpyridineplatinum(II) complex, also

* Corresponding author. Instituto de Química, Universidade Federal de Uberlândia, Av. João Naves de Ávila, 2121, Campus Santa Mônica, 38, Uberlândia, MG, Brazil.
** Corresponding author. Instituto de Química, Universidade Federal de Uberlândia, Av. João Naves de Ávila, 2121, Campus Santa Mônica, 38, Uberlândia, MG, Brazil.
E-mail addresses: paixaodrielly@hotmail.com (D.A. Paixão), wendell.guerra@ufu.br (W. Guerra).

https://doi.org/10.1016/j.cinorg.2024.100049
Received 9 January 2024; Received in revised form 24 April 2024; Accepted 25 April 2024
Available online 3 May 2024

called picoplatin, which was developed to overcome development of resistance to other Pt-based drugs [11,12]. Picoplatin showed high anticancer activity *in vitro* and *in vivo*, as well as in several advanced clinical trials in patients suffering from, for example, small-cell lung cancer [13]. In another studies, a series of [Pt(*cis*-1,3-diaminocycloalkane)Cl_2] complexes were prepared and the analogue containing the cyclobutyl moiety showed significant antiproliferative activity in tumor cells, besides the hallmarks typical of immunogenic cell death (ICD) inducers [14]. Platinum(II) complexes with benzyliminoether derivatives were evaluated in terms of cell growth inhibition against several types of human cancer cell lines. One of them, the *cis*-[$PtCl_2${E-N(H)C(OMe)CH_2Ph}$_2$] complex was significantly more potent than cisplatin against all tumor cell lines evaluated, showing IC_{50} values from about 2- to 17-fold lower than the cisplatin. In addition, this complex induced apoptosis in a dose-dependent manner, accompanied by the activation of caspase-3 [15]. Farrell et al. synthesized platinum(II) complexes with bulky amine ligands that exhibited activity against both cisplatin resistant and sensitive cell lines [16]. Lastly, another interesting example is the complex [Pt(3-aminoflavone)$_2Cl_2$] that showed cytotoxicity against human and murine cancer cell lines. Furthermore, it proved to be much less toxic for normal lymphocytes in comparison to cisplatin, which reduces the number of potential adverse effects. Additionally, biochemical and morphological methods showed that the proapoptotic activity of [Pt(3-aminoflavone)$_2Cl_2$] is markedly higher than that of cisplatin [17].

The results described above clearly show that platinum complexes having a [$PtCl_2(L)_2$] (L = *N*-donor ligand) chemotype can be useful as anticancer agents. Thus, we have designed a new platinum(II) complex containing bda that is easily prepared and very stable. Subsequently, their modes of interaction with DNA were studied and their anticancer effects against breast cancer cell lines were evaluated. Surprisingly, we have not found any studies in the literature involving 1,4-benzodioxan-6-amine acting as a ligand.

2. Experimental section

2.1. Starting materials

$K_2[PtCl_4]$ and 1,4-benzodioxan-6-amine were purchased from Sigma-Aldrich. All other chemicals reagents and solvents were of analytical grade, purchased from different sources, and used without prior purification.

2.2. Synthesis of the complex [$PtCl_2(bda)_2$]

To an aqueous solution of $K_2[PtCl_4]$ (0.25 mmol, 0.1037g) was added dropwise 0.50 mmol of bda (0.0756g) dissolved in a minimum amount of methanol. Next, the mixture was stirred for 24 h at room temperature. After this time, a solid was filtered, washed with distilled water, methanol and ethyl ether and dried under reduced pressure.

Yield: 86.42 %. Color: Grayish brown. Molar weight (g mol^{-1}): 568.315. Anal. Calc. for [$PtCl_2(C_8H_9NO_2)_2$]: C, 33.81; H, 3.19; N, 4.93 %; Found: C, 33.71; H, 3.06; N, 4.88 %. ^{1}H NMR (400 MHz; DMF-d_7) δ (ppm): 4.25–4.29 (m, CH_2–O, H7, H8); 6.67 (d, ^3J = 8.5 Hz, CH, H4); 6.69 (dd, ^3J = 8.6 Hz, ^4J = 2,6 Hz, CH, H5); 6.93 (d, ^4J = 2.6 Hz, CH, H1); 7.06 (s, NH_2). ^{13}C NMR (100 MHz; DMF-d_7) δ (ppm): 63.8 (C8); 64.0 (C7); 111.7 (C1); 115.4 (C5); 116.0 (C4); 135.1 (C3); 140.9 (C6); 142.7 (C2). ^{195}Pt NMR (86 MHz; DMF-d_7) δ (ppm): −2073. ^{195}Pt NMR (86 MHz; DMSO-d_6) δ (ppm): - 2065. IR spectra in ATR, ν (cm^{-1}): 3243-3184 (νNH_2), 3055-2862 (νCH), 1063 (νsC–O–C), 335-321(νPt–Cl). UV–Vis (ACN), λmax(ε) = 290 (8.25 × 10^3 M^{-1} cm^{-1}), 255 (8.41 × 10^3 M^{-1} cm^{-1}), 224 (2.68 × 10^4 M^{-1} cm^{-1}) nm. Molar conductivity, Λ_M, (DMSO) = 0.99 S cm^2 mol^{-1}.

2.3. Physical measurements

Molar conductivity measurement was carried out in DMSO (10^{-3} M) with tetramethylammonium bromide (ΛM = 79.12 S cm2 mol-1) as a standard, using a Tecnal Tec-4MP conductivity meter. Microanalyses of C, H and N were performed in a CHNSO PerkinElmer 2400 Analyzer. IR spectra (4000–220 cm^{-1}) were obtained on a PerkinElmer Frontier MIR spectrometer equipped with an attenuated total reflectance (ATR) sample holder with a diamond crystal. UV–Vis spectra were obtained on a Shimadzu UV-2501 PC spectrophotometer. The TGA/DTA curves were obtained on a Shimadzu thermobalance, model DTG-60H, using an aluminum crucible. For this, 6 mg of complex were heated at 10 °C min^{-1} from room temperature to 600 °C, in a dynamic nitrogen atmosphere (flow rate of 50 mL min^{-1}). NMR spectra were recorded on a Bruker spectrometer and were obtained by dissolving the platinum complex in DMF-d_7 (^{1}H, ^{13}C and ^{195}Pt) or DMSO-d_6 (^{195}Pt), depending on the study. The chemical shifts were expressed as δ (in ppm) from internal reference standard TMS (^{1}H and ^{13}C NMR) and K_2PtCl_6 (^{195}Pt NMR).

2.4. Cytotoxic activity

The cell viability was assessed by the MTT method as proposed by Mosmann [18]. Herein, 5.0 × 10^5 cells (MCF-7 or MDA-MB231) were incubated for 24 h in 96-well plates. After this incubation period, the complex, bda or cisplatin (positive control) was added (concentration from 500 μM to 3.90 μM in serial dilution; compounds solubilized in 0.5 % DMF) in a final volume of 200 μL. Cells were incubated for 48 h at 37 °C. After incubation with the compounds, the medium was removed and 50 μL of MTT (2.0 mg mL^{-1}) diluted in phosphate buffered saline (PBS) was added. The precipitate blue MTT formazan was then dissolved in 50 μL of DMF, and the absorbance was measured at 570 nm in a VARIAN CARY-50 plate reader MPR multiwell. Cell viability was expressed as the percentage of absorption values in treated cells compared to untreated (control) cells. The adjustment of the IC_{50} curve was performed using the GraphPad Prism 5 software (GraphPad Software Inc., San Diego, CA).

2.5. DNA binding studies

2.5.1. DNA solution

The Calf thymus (CT) DNA solution was freshly prepared in 5.0 × 10^{-3} M Tris–HCl and 50 × 10^{-3} M NaCl in pH 7.3. The CT-DNA concentrations was determined spectrophotometrically with ε = 6600 M^{-1} cm^{-1} at 260 nm, ratio UV absorbance at 260 and 280 nm. CT-DNA was free of proteins because, the ratio between 260 nm and 280 nm absorption bands (A_{260}/A_{280}) was found between 1.80 and 1.91 [19]. CT-DNA was purchased from Sigma Chemical Co. (USA) and used as received.

2.5.2. Circular dichroism (CD) spectroscopy

CD spectra were recorded in the range 235–320 nm on a JASCO J-815 spectropolarimeter with 5 accumulations and scanning speed of 100 nm/min, using a 0.1 cm path length quartz cuvette at room temperature. The CT-DNA solution (Tris-HCl buffer 5.0 × 10^{-3} M/NaCl 50 × 10^{-3} M, pH = 7.3) was prepared at a concentration of 50 × 10^{-6} M. The stock solutions were prepared in dimethylformamide (DMF) and the complex concentration varied from 0 to 20 × 10^{-6} M. The samples were prepared with the [complex]/[DNA] molar ratios from 0 to 0.3 and incubated for 48 h at 310 K.

2.5.3. DNA spectroscopic titration

The electronic spectra were recorded on a Thermo Scientific Evolution Array UV–Visible Spectrophotometer at room temperature. In UV–Vis absorption titration experiments were used a quartz cell of 10

mm path length with Tris-HCl buffer and 2 % DMF. The concentration of platinum complex was fixed at (2.0×10^{-6} M) and the electronic spectra were recorded after each addition of CT-DNA (molar ratios from 0 to 3.0). Spectral changes in absorbance were monitored at the maximum wavelengths of 288 for the complex. The intrinsic equilibrium binding constant (K_b) of complex to CT-DNA was obtained by the Benesi-Hildebrand equation [20].

$$\frac{A_0}{A - A_0} = \frac{\varepsilon_G}{\varepsilon_{H-G} - \varepsilon_G} + \frac{\varepsilon_G}{\varepsilon_{H-G} - \varepsilon_G} \times \frac{1}{K_b[DNA]}$$

Where A an A_0 are absorbance of the complex solution in the presence and absence of CT-DNA, respectively. ε_G and $\varepsilon_{H\text{-}G}$ are the molar absorptivity coefficients of the free complex and complex–CT-DNA, respectively. The K_b constant was determined by the ratio between the linear and angular coefficient from the plot of $A_0/(A\text{-}A_0)$ versus 1/[DNA].

2.5.4. Hoechst 33258 displacement assay

Fluorescence spectra were recorded in range 358–660 nm, with excitation wavelength of 338 nm, 5.0 nm bandwidth and room temperature on a fluorescence accessory of the Jasco spectropolarimeter (J-815), using a quartz cell of 10 mm path length. DNA and Hoechst 33258 concentrations were fixed in 60×10^{-6} M and 6.0×10^{-6} M, respectively and titrated with successive aliquots of complex in DMF ($0 - 60 \times 10^{-6}$ M).

2.6. Flow cytometer assay

To evaluate the apoptosis, MCF-7 cells were screened in 12- well plates at 5.0×10^6 cell/well for 24 h. Next, they were treated with $[PtCl_2(bda)_2]$ or cisplatin as positive control for 48 h. Thereafter, the cells were tripsinized, washed with ice cold PBS and resuspended in binding buffer, according to the kit instructions. The cells were then incubated with FITC-conjugated Annexin V (1:100) for another 15 min as recommended by FITC Annexin V Apoptosis Detection Kit (BD PharmingenTM). Propidium iodide (1 μg/mL) was added immediately before BD FAXCANTOTM flow cytometer analysis. The excitation/emission was 582/617 nm. A total of 10,000 events were counted per sample, and analyzed by software BD FACSDIVA (BD System).

2.7. In vitro wound healing assay

To investigate wound healing potential of $[PtCl_2(bda)_2]$, we performed scratch wound healing assay. In brief, 5.0×10^5 MCF-7 cells per well were seeded in 24-well plates and were grown to reach confluent monolayer. Then using a 200 μl pipette tip, the scratches were created. Cells were washed three times with PBS and treated with 10 μM of cisplatin (positive control) and $[PtCl_2(bda)_2]$. After 48h after the creation of wounds, three different areas were images through Axiovert 200 M. Wound healing distances were measured and expressed as the average percent of wound closure by comparing the zero time.

3. Results and discussion

Under mild conditions and with good yield, a new platinum(II) complex was prepared by the reaction of $K_2[PtCl_4]$ with 1,4-benzodioxan-6-amine (bda). The isolated complex (Fig. 1) is very soluble in DMF and DMSO and was characterized by molar conductivity, elemental and thermal analysis (TGA/DTA), UV–Vis, FT-IR and ^1H, ^{13}C and ^{195}Pt NMR.

The elemental analysis data (C, H and N) are in accordance with the molecular formula $[PtCl_2(C_8H_9NO_2)_2]$. A freshly prepared solution of the complex in DMSO exhibited a molar conductivity value far below the 1:1 standard electrolyte, indicating that the complex behaves as a nonelectrolyte [21,22]. The thermal stability of the complex was evaluated in the temperature range of 25–600 °C. As can be seen in Fig. 2, endothermic

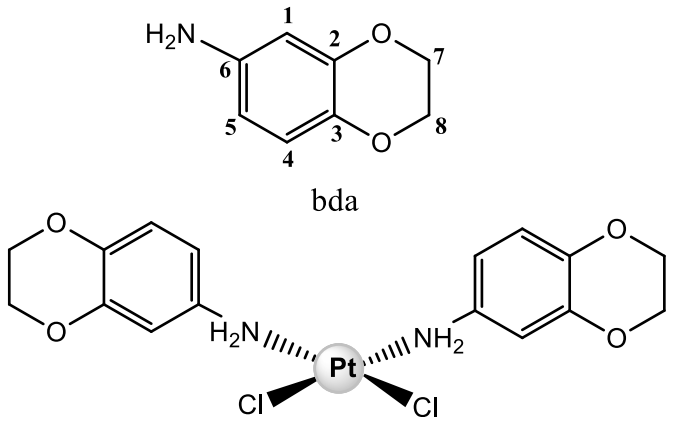

Fig. 1. 1,4-benzodioxan-6-amine (bda) and proposed structure for $[PtCl_2(bda)_2]$.

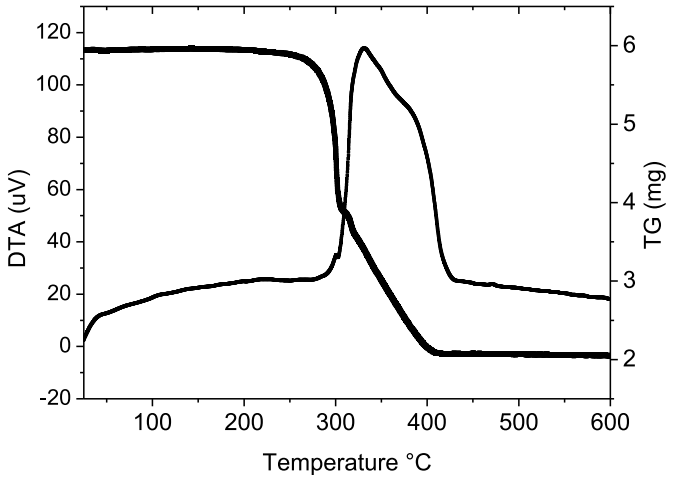

Fig. 2. TG/DTA curves for $[PtCl_2(bda)_2]$.

events between 200 and 500 °C are due to thermal decomposition of the complex. At 600 °C there is a residue (elemental platinum) corresponding to 34.39 % (Calculated: 34.33 %), corroborating the proposed structure, since the percentage of metal fits well with the proposed formula [23]. The TG curve also reveals a high thermal stability for the sample, since no weight loss was observed in the TG curve up to 200 °C.

The UV–Vis spectra of bda and its platinum complex were performed in acetonitrile (10^{-5} M). As can be seen in Fig. 3, bda exhibited three bands between 200 and 400 nm that can be assigned to n→π and π→π* transitions (ILCT). In the spectrum of the complex, a red or blue shift in comparison to the free ligand confirms its presence in solution [24].

As to the FT-IR spectra (see Fig. S1), bda exhibits two characteristic absorptions in the range of 3351 to 3222 cm^{-1} that can be assigned to νNH_2. The vibrational frequencies between 3055 and 2872 cm^{-1} are due to aromatic and aliphatic CH groups. An absorption band around 1063 cm^{-1} can be attributed to νs(C–O–C) [25]. In the FT-IR spectrum of $[PtCl_2(bda)_2]$, the absorption bands corresponding to νNH_2 showed considerable shift in relation to the free ligand, corroborating the coordination of the amino group to the metal ion. New absorptions close to 335 and 321 cm^{-1} can be assigned to νPt–Cl stretching, which suggests a *cis* geometry [26].

The nuclear magnetic resonance (NMR) spectra were recorded in DMF-d_7. In the ^1H NMR spectrum of the uncoordinated ligand, the NH_2 protons appeared as a singlet at δ 4.69. In the spectrum of complex, this signal was significantly shifted downfield (δ 7.06), suggesting coordination through the nitrogen atom. The resonances related to other

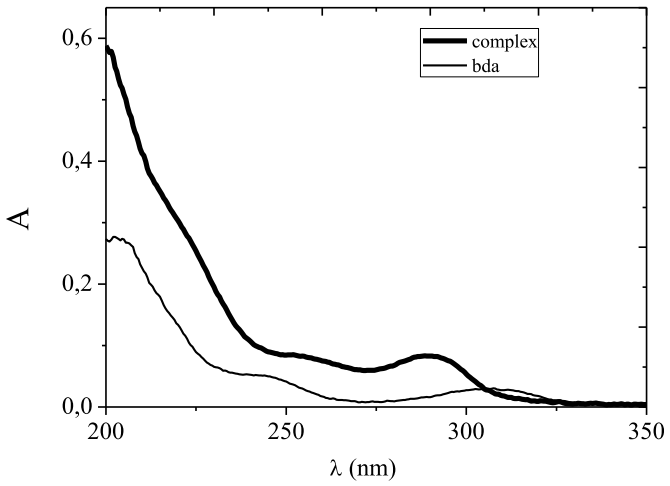

Fig. 3. UV–Vis spectra of bda and its platinum complex (ACN, 10^{-5} M).

protons (see the experimental section) were only slightly affected, which reinforces the involvement of nitrogen in coordination. Analyzing the ^{13}C NMR spectrum of the uncoordinated ligand, it was possible to observe eight signals at 63.60, 64.19, 102.26, 107.10, 116.56, 134.44, 143.07 and 143.50 ppm attributable to the carbons C8, C7, C1, C5, C4, C3, C2 and C6, respectively. In the ^{13}C NMR spectrum of the complex, only the signals assigned to carbons C1 (111.7 ppm), C5 (115.4 ppm) and C6 (140.9 ppm) showed considerable changes, which also suggests coordination through the nitrogen atom. As to the ^{195}Pt NMR spectrum, a signal at δ −2073 is in the expected range for platinum(II) with an N_2Cl_2 coordination environment [27].

3.1. Stability

The behaviour of the complex in aqueous solutions (containing 1 % DMSO or DMF) was investigated by molar conductivity measurements over a period of 48 hs. In all cases, the conductivity values found revealed a non-electrolytic behaviour for the complex, suggesting that both chlorides remain coordinated to platinum.

The stability of $[PtCl_2(bda)_2]$ was also determined by ^{195}Pt NMR over 72 h at room temperature. According to the experiments performed, we can conclude that the complex is stable in pure DMSO for at least 20 min (Fig. S2). However, after 20 min, in addition to the signal at δ −2065, a new signal appeared at δ −2982, probably due to the replacement of a bda ligand by a DMSO molecule, producing $[PtCl_2(bda)(DMSO)]$. This proposal is in agreement with the conductivity experiments discussed above. Subsequently, another signal appeared within 2 h (Pt signal, −3094 ppm) and may be attributed to a *cis-trans* equilibrium involving $[PtCl_2(bda)(DMSO)]$ [28,29]. Within 12 h at room temperature, the complex $[PtCl_2(bda)_2]$ was completely consumed, as is evident from the disappearance of signal at δ −2065. Despite the solvolysis in pure DMSO, the complex is very stable in pure DMF as verified by ^{195}Pt NMR over a period of 72 h, where only a signal close to δ −2073 was observed (Fig. S3).

Additionally, the stability of complex was also investigated by UV–Vis in a PBS buffer solution containing 1 % DMSO or DMF at 37 °C. A band located at 288 nm allowed the monitoring of the solution behaviour of this complex. Thus, as can be seen in Fig. S4, the absorption band at 288 nm remains unchanged in the first 2 h and gradually increase in the last (between 4 and 48 h), indicating that complex undergoes solvolysis in DMSO, according to the results discussed above. On the other hand, in PBS buffer solution containing 1 % DMF, the UV–Vis spectral data (Fig. S5) reveals that the band located around 288 nm was not affected over a period of 48 h, indicating no dissociation (loss of bda ligand) of this complex. Furthermore, no change in color of the solution or formation of precipitate was observed during the experiment.

3.2. Cytotoxic activity

To assess the potential *in vitro* antitumor activity of bda and its platinum(II) complex, we evaluated their cytotoxic effects against two breast cancer cell lines (MCF-7 and MDA-MB-231) and in a non-tumor cell line (MCF-10) using the MTT method. Thus, IC_{50} values were determined for each cell line cultured after 48 h of continuous exposure to compounds. Cisplatin was used as a positive control and we have checked that the solvent had no effect on cell growth.

Analyzing the data (Table 1), it is possible to verify that the platinum complex showed greater cytotoxic activity against the MCF-7 breast cancer cell line when compared to free ligand and cisplatin. More specifically, in the MCF7 cell line, the complex ($IC_{50(MCF\text{-}7)}$ = 17.33 μM) was approximately 2.3 times more effective than free bda ($IC_{50(MCF\text{-}7)}$ = 40.28 μM) and about 3.4 times more active than cisplatin ($IC_{50(MCF\text{-}7)}$ = 58.27 μM). As to the MDA-MB-231 cell line, the complex ($IC_{50(MDA\text{-}MB231)}$ = 56.60 μM) was slightly more effective than free ligand ($IC_{50(MB231)}$ = 73.55 μM) and as active as cisplatin ($IC_{50(MB231)}$ = 53.32 μM). When compared to platinum(II) complexes containing amines and chlorides tested against breast cancer cell lines, $[PtCl_2(bda)_2]$ is among the most potent [30–34] and has been shown to be a potential candidate against breast cancer. In fact, the results reported here are relevant, since breast cancer is the most common among women, being that some subtypes have high metastatic potential and limited pharmacological treatment [35–38].

3.3. DNA binding studies

DNA is the main pharmacological target of cisplatin and its analogues [39]. Taking this into account, the interaction of the complex with CT-DNA has been studied by several spectroscopic methods. Titration of metal complexes with DNA and monitoring their UV–Vis absorption spectra can provide important clues about their mode of interaction. Binding of an intercalating molecule to DNA is suggested a hypochromic effect accompanied by bathochromism (red shift) [40,41]. Compound $[PtCl_2(bda)_2]$ exhibits an intraligand charge transfer (ILCT) band at 290 nm which may be perturbed in the presence of DNA. Fig. 4 shows the electronic spectrum of the complex $[PtCl_2(bda)_2]$. On increasing CT-DNA concentration, it was noticed a hypochromic effect on the ILCT absorption of complex close to 290 nm. The calculated binding constant K_b value was 1.06×10^3 M^{-1} (correlation coefficient (R) = 0.9888). This value is lower than the binding constants values reported for classical intercalators and metallointercalators (10^5–10^7 M^{-1}) [39].

Circular dichroism (CD) spectroscopy is a powerful technique that is widely used to evaluate modifications of the DNA secondary structure induced by metal complexes binding [42,43]. In the region at 230–300 nm, the typical CD spectra of the CT-DNA exhibits two bands, one

Table 1
Cytotoxic activity of the platinum(II) complex, bda and cisplatin against breast cell lines.

Compounds	IC_{50} (μM)		
	MFC-10	MFC-7	MDA-MB-231
$[PtCl_2(bda)_2]$	44.78 ± 3.1	17.33 ± 1.1	56.60 ± 0.07
bda	69.20 ± 4.2	40.28 ± 2.9	73.55 ± 4.4
cisplatin	92.62 ± 3.1	58.27 ± 3.1	53.32 ± 4.6

Legends to the Figures.

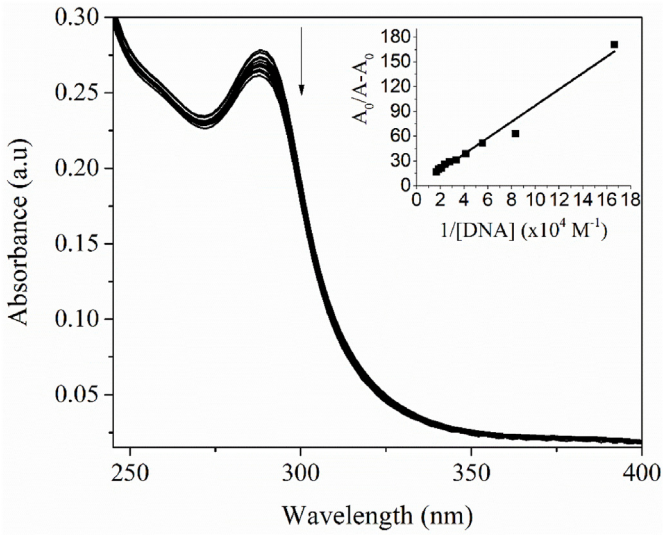

Fig. 4. UV–Vis absorption spectra of solutions (pH = 7.3) containing the complex (20×10^{-6} M) and increasing concentrations of CT-DNA. Insert: A0/A-A0 versus 1/[DNA].

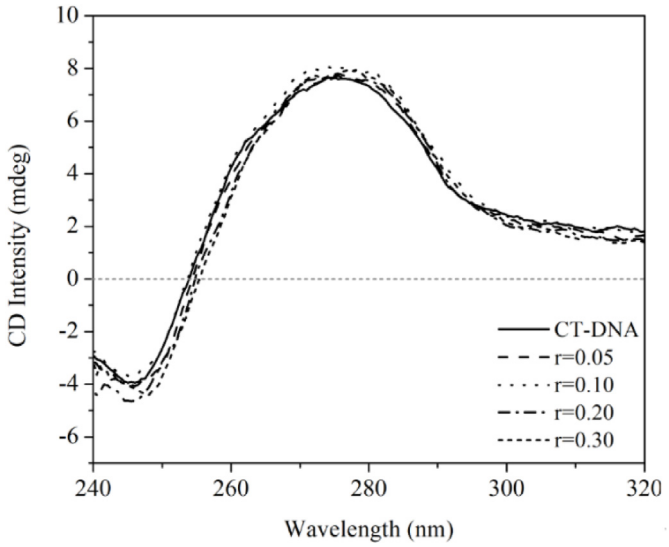

Fig. 5. CD spectra after addition of increasing of complex (1.0×10^{-3} M, DMF) to CT-DNA (50×10^{-6} M) in Tris-HCl buffer 5×10^{-3} M/NaCl 50×10^{-3} M, r = molar ratio concentrations [complex]/[DNA].

positive at ~275 nm and other negative at ~245 nm attributed to the stacking of DNA pairs bases and the right-handed B form DNA, respectively [42]. An increase in the ellipticy of both bands is indicative of intercalation. On the other hand, little or no change in CD spectra suggests groove binding or electrostatic interaction [43]. Fig. 5 shows CD spectrum of complex. On increasing the concentration of the platinum complex, few or no significant change on CD spectral profile was noticed, suggesting an electrostatic interaction and/or groove binding.

The competitive displacement assay with bis-benzimidazole (Hoechst 33258) was performed to obtain more information about the binding mode involved between the platinum complex and CT-DNA. Hoechst 33258 is a fluorescence probe that binds with high selectivity to minor groove of DNA structure. The binding of this probe leads to a significant increase of fluorescence intensity of DNA-Hoechst system [44]. Fluorescence quenching is observed when a compound is able to release Hoechst 33258 from DNA structure [11]. In addition, Hoechst can also be released by other molecules which are able to bind in other sites of DNA

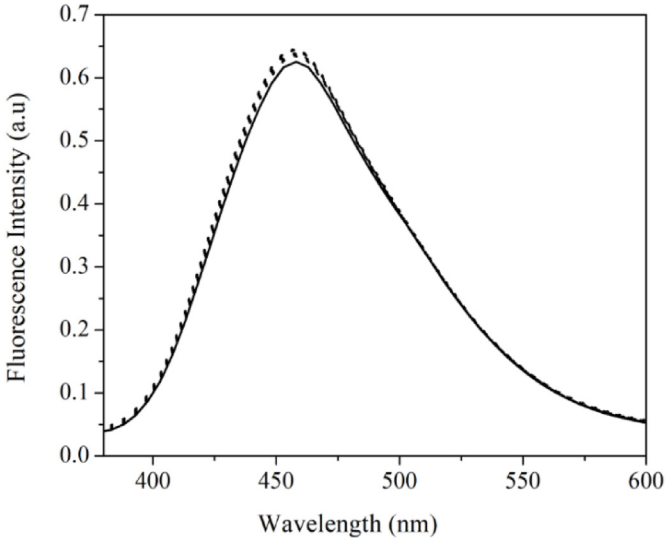

Fig. 6. Fluorescence spectra of the Hoechst-DNA systems in aqueous buffer in absence and presence of increasing amounts of complex. λ_{ex} = 338 nm, [Hoechst] = 6.0×10^{-6} M, [DNA] = 60×10^{-6} M, [Complex] = 0–60×10^{-6}.

[45]. Fig. 6 shows fluorescence spectrum of complex.

On increasing the concentration of the platinum complex, no quenching is observed, suggesting that the complex is not capable of release the Hoechst 33258 from DNA structure. This finding suggests that the platinum complex is not able to bind to the DNA minor groove. Nevertheless, another non-intercalative binding mode cannot be ruled out.

3.4. Flow cytometer assay and in vitro wound healing potency

As platinum (II) complex showed cytotoxic potency against MCF-7 tumor cells, we evaluated what was the signaling way that $[PtCl_2(bda)_2]$ leads the breast cancer cell to death. For this, MCF-7 cells were treated with cisplatin (positive control) and platinum(II) complex for 48 h. Tumor cells were then stained with Annexin V and PI (iodide of propidium) simultaneously and analyzed for early apoptosis, late apoptosis or necrosis signaling pathway cells (Fig. 7A). The treatment with $[PtCl_2(bda)_2]$ leads to a discrete necrosis, approximately 15 % in 48 h of assay (Fig. 7A). In this time, the most viable cells have not entered death pathways showing a high potential of viability at a lower dose of treatment. Under the same conditions, the cisplatin treatment showed both early (32 %) and late (approximately 30 %) apoptosis of MCF-7 cells (Fig. 7B and C).

For further examination, we measured migration capacity of platinum(II) complex treated MCF-7 cells by *in vitro* scratch wound healing assay (Fig. 8A). $[PtCl_2(bda)_2]$ treatment displayed significantly delayed wound closure as compared as cisplatin or the negative control treatment (Fig. 8B), importantly to invasive and metastasis characteristic of this MCF-7 cells. MCF-7 expressed E-cadherin, vimentin and fibronectin which are closely related to the migratory and invasive capacity of these cells [46]. Further studies may demonstrate the mechanisms by platinum(II) complex can help inhibit cell migration and serve as an adjuvant in the treatment of breast cancer.

4. Concluding remarks

A new platinum(II) complex was prepared and characterized by physicochemical and spectroscopic methods. The coordination sphere of the platinum ion is occupied by two chlorides and two amine ligands, which coordinate to the platinum ion through the nitrogen atom. The complex interacted with DNA and exhibited cytotoxic activity against the

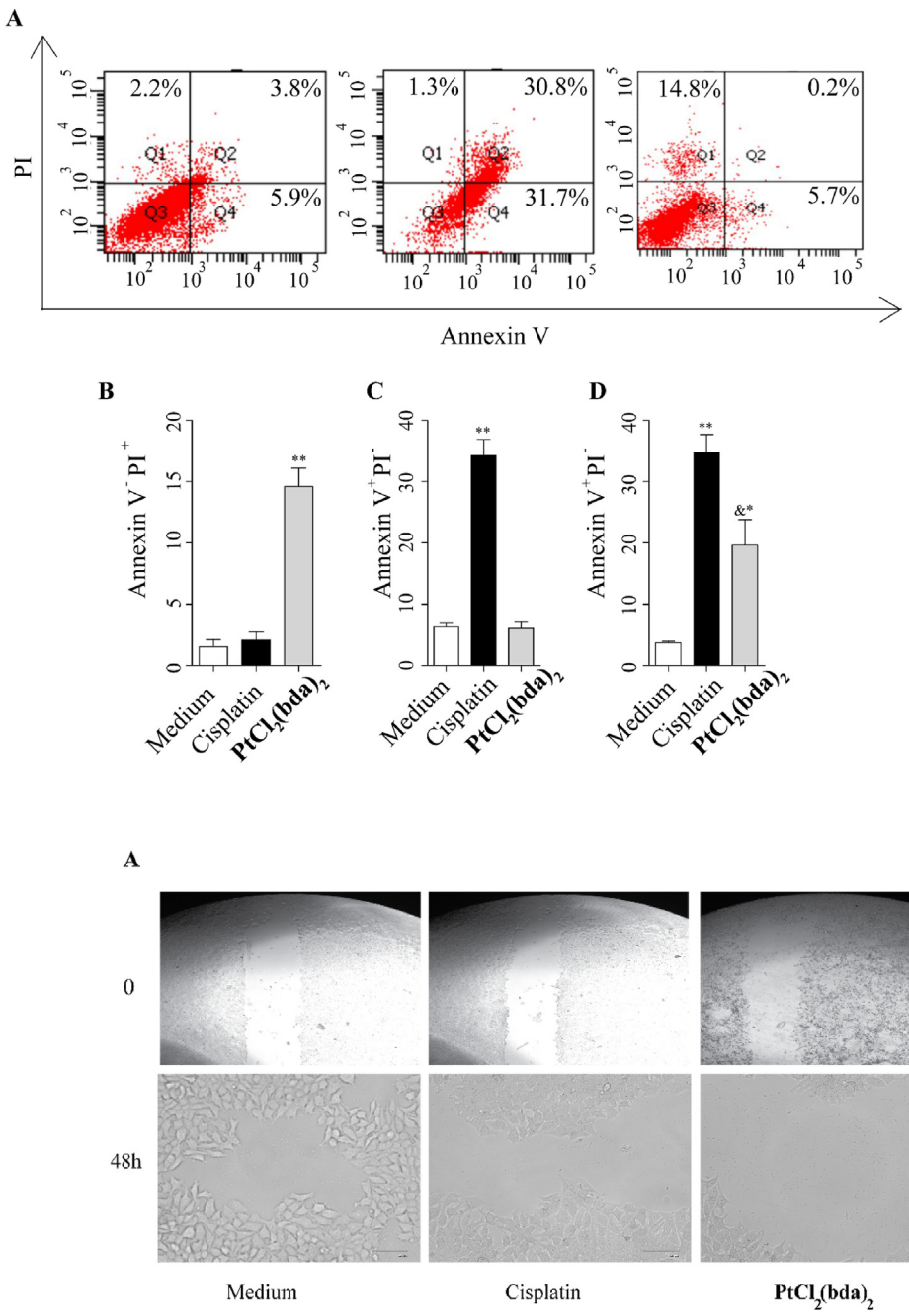

Fig. 7. Platinum(II) complex maintained the viability of MCF-7 cells and leads to discrete necrosis pathway. Dot plot of Annexin V, PI stain in MCF-7 treat with medium, cisplatin and $[PtCl_2(bda)_2]$ (**A**). Treatment with $[PtCl_2(bda)_2]$ leads to discrete necrosis (B), but not to induces to early (C) or late apoptosis. Results presented as the mean of triplicated experiments. Student's *t*-test and nonparametric data were compared with Mann-Whitney *U* test. Significant differences compared to the medium are denoted * $p < 0.05$ or ** $p < 0.01$ and compared to the cisplatin are denoted $^{\&}p < 0.05$.

Fig. 8. Migratory abilities of MCF-7 cell in wound healing assay. (**A**) Optical microscopic images of *in vitro* wound healing at 0 h and 48 h after the creation of wounds. (**B**) Comparison of images to quantify the migration rate of the cells. Wound distances were measured at each time point and expressed as percent wound closure by comparing b zero time. Data are the means ± SD (n = 3). Statistical analysis was performed by Student's test, *$p < 0.05$ and ***$p < 0.001$ compared the cisplatin and platinum compounds with medium treatment.

MCF-7 and MDA-MB-231 tumor cell lines. Considering the high metastatic potential and limited pharmacological treatment for some types of breast cancer, the complex reported here represents a starting point for new synthesis and biological studies.

CRediT authorship contribution statement

Meiry L. Lacerda: Methodology, Investigation, Formal analysis. **Carla D. Lopes:** Writing – review & editing, Writing – original draft, Methodology, Investigation, Formal analysis, Data curation. **Raphael T.C. Silva:** Methodology, Investigation, Formal analysis, Data curation. **Renan D. Zanetti:** Investigation, Methodology, Validation. **Mariete B. Moreira:** Formal analysis, Investigation, Methodology, Supervision, Validation, Writing – original draft, Writing – review & editing. **Adelino V.G. Netto:** Formal analysis, Funding acquisition, Investigation, Methodology, Project administration, Supervision, Validation, Writing – original draft, Writing – review & editing. **Wesley A. Souza:** Methodology, Investigation, Formal analysis, Data curation. **Sérgio de Albuquerque:** Funding acquisition, Methodology, Project administration, Supervision. **Drielly A. Paixão:** Writing – review & editing, Writing – original draft, Validation, Methodology, Investigation, Formal analysis, Data curation. **Wendell Guerra:** Writing – review & editing, Writing – original draft, Visualization, Validation, Supervision, Project administration, Investigation, Funding acquisition, Formal analysis, Data

curation, Conceptualization.

Declaration of competing interest

The authors declare that they have no known competing financial interests or personal relationships that could have appeared to influence the work reported in this paper.

Acknowledgements

We thank FAPEMIG (Fundação de Amparo à Pesquisa de Minas Gerais, Brazil), CNPq (Conselho Nacional de Desenvolvimento Científico e Tecnológico, Brazil) and CAPES (Coordenação de Aperfeiçoamento de Pessoal de Nível Superior) for financial support and grants. W. Guerra thanks CNPq for grant number 303210/2021-4. The authors are also grateful for the financial support provided by FAPESP (proc. 2022/14041-0).

Appendix A. Supplementary data

Supplementary data to this article can be found online at https://doi.org/10.1016/j.cinorg.2024.100049.

Abbreviations

ACN	Acetonitrile
UV–Vis	Ultraviolet–visible spectroscopy
FT-IR	Fourier-transform infrared spectroscopy
NMR	Nuclear magnetic resonance spectroscopy
CD	circular dichroism
ct-DNA	calf thymus DNA
DMF	dimethylformamide
DMSO	dimethylsulfoxide

References

[1] Q. Zhang, Q.B. Lu, New combination chemotherapy of cisplatin with an electron-donating compound for treatment of multiple cancers, Sci. Rep. 11 (2021) 788, https://doi.org/10.1038/s41598-020-80876-z.
[2] E. Rossini, V. Bosatta, A. Abate, M. Fragni, V. Salvi, R.M. Basnet, D. Zizioli, D. Bosisio, G. Piovani, F. Valcamonico, G. Mirabella, A. Berruti, M. Memo, S. Sigala, Cisplatin cytotoxicity in human testicular germ cell tumor cell lines is enhanced by the CDK4/6 inhibitor palbociclib, Clin. Genitourin. Cancer 19 (2021) 316–324, https://doi.org/10.1016/j.clgc.2021.01.006.
[3] Y. Lugones, P. Loren, L.A. Salazar, Cisplatin resistance: genetic and epigenetic factors involved, Biomolecules 12 (2022) 1365, https://doi.org/10.3390/biom12101365.
[4] D. Gibson, Platinum(IV) anticancer agents; are we en route to the holy grail or to a dead end? J. Inorg. Biochem. 217 (2021) 111353 https://doi.org/10.1016/j.jinorgbio.2020.111353.
[5] A. Khoury, K.M. Deo, J.R. Aldrich-Wright, Recent advances in platinum-based chemotherapeutics that exhibit inhibitory and targeted mechanisms of action, J. Inorg. Biochem. 207 (2020) 111070, https://doi.org/10.1016/j.jinorgbio.2020.111070.
[6] P. Yue, B. Han, Y. Zhao, Focus on the molecular mechanisms of cisplatin resistance based on multi-omics approaches, Mol. Omics 19 (2023) 297–307, https://doi.org/10.1039/D2MO00220E.
[7] A.R.S. Fernandes, G. Alves de Brito, A.L. Baptista, L.A.S. Andrade, M.H. Imanishe, B.J. Pereira, The influence of acute kidney disease on the clinical outcomes of patients who received cisplatin, carboplatin, and oxaliplatin, Health Sci Rep 5 (2022) e479, https://doi.org/10.1002/hsr2.479.
[8] J. Małyszko, K. Kozłowska, L. Kozłowski, J. Małyszko, Nephrol. Dial. Transplant. 32 (2017) 924–936.
[9] H.H. Hsu, M.C. Chen, R. Baskaran, Y.M. Lin, C.H. Day, Y.J. Lin, C.C. Tu, V. Vijaya Padma, W.W. Kuo, C.Y. Huang, J. Cell. Physiol. 233 (2018) 5458–5467.
[10] Z. Jiabei, K. Yu, C. Lu, W. Hua, L. Junqing, Z. Su, Y. Lushan, The drug-resistance mechanisms of five platinum-based antitumor agents, Front. Pharmacol. 11 (2020) 343, https://doi.org/10.3389/fphar.2020.00343.
[11] G. Facchetti, I. Rimoldi, Anticancer platinum(II) complexes bearing N-heterocycle rings, Bioorg. Med. Chem. Lett 29 (2019) 1257–1263, https://doi.org/10.1016/j.bmcl.2019.03.045.
[12] C.H. Tang, C. Parham, E. Shocron, G. McMahon, N. Patel, Picoplatin overcomes resistance to cell toxicity in small-cell lung cancer cells previously treated with cisplatin and carboplatin, Cancer Chemother. Pharmacol. 67 (2011) 1389. https://doi-org.ez34.periodicos.capes.gov.br/10.1007/s00280-010-1435-5.
[13] P. Štarha, B. Drahoš, R. Herchel, An unexpected in-solution instability of diiodido analogue of picoplatin complicates its biological characterization, Dalton Trans. 50 (2021) 6071–6075.
[14] V. Novohradsky, L. Markova, H. Kostrhunova, J. Kasparkova, J. Hoeschele, V. Brabec, A [Pt(*cis*-1,3-diaminocycloalkane)Cl_2] analog exhibits hallmarks typical of immunogenic cell death inducers in model cancer cells, J. Inorg. Biochem. (2021) 111628, https://doi.org/10.1016/j.jinorgbio.2021.111628.
[15] S.M. Sbovata, F. Bettio, M. Mozzon, R. Bertani, A. Venzo, F. Benetollo, R.A. Michelin, V. Gandin, C. Marzano, Cisplatinum and transplatinum complexes with benzyliminoether ligands; synthesis, characterization, Structure−Activity relationships, and *in vitro* and *in vivo* antitumor efficacy, J. Med. Chem. 50 (2007) 4775–4784.
[16] N. Farrell, T.T.B. Ha, J.P. Souchard, F.L. Wimmer, S. Cros, N.P. Johnson, Cytostatic *trans*-platinum(II) complexes, J. Med. Chem. 32 (1989) 2240–2241, https://doi.org/10.1021/jm00130a002.
[17] M. Fabijańska, K. Studzian, L. Szmigiero, A.J. Rybarczyk-Pirek, A. Pfitzner, B. Cebula-Obrzut, P. Smolewski, E. Zynera, J. Ochocki, *Trans*-Platinum(II) complex of 3-aminoflavone – synthesis, X-ray crystal structure and biological activities *in vitro*, Dalton Trans. 44 (2015) 938–947, https://doi.org/10.1039/C4DT01501K.
[18] T. Mosmann, Rapid colorimetric assay for cellular growth and survival: application to proliferation and cytotoxicity assays, J. Immunol. Methods 65 (1983) 55–63.
[19] G.H. Ribeiro, L. Colina-Vegas, J.C.T. Clavijo, J. Ellena, M.R. Cominetti, A.A. Batista, Ru(II)/N-N/PPh 3 complexes as potential anticancer agents against MDA-MB-231 cancer cells (N-N = diimine or diamine), J. Inorg. Biochem. 193 (2019) 70–83.
[20] W. Villarreal, L. Colina-Vegas, G. Visbal, O. Corona, R.S. Corrêa, J. Ellena, M.R. Cominetti, A.A. Batista, M. Navarro, Copper(I)-Phosphine polypyridyl complexes: synthesis, characterization, DNA/HSA binding study, and antiproliferative activity, Inorg. Chem. 56 (2017) 3781–3793.
[21] M.A. Rodrigues, I.M. Marzano, G.H. Ribeiro, L. Colina-Vegas, M. Pivatto, A.P.S. Fontes, C.M. Ribeiro, F.R. Pavan, K.J. de Almeida, A.A. Batista, E.C. Pereira-Maia, W. Guerra, Platinum(II) complexes with carbazates and hydrazides: synthesis, spectral characterization, computational modeling, and biological studies, Polyhedron 98 (2015) 146–153, https://doi.org/10.1016/j.poly.2015.06.025.
[22] G.D. de Souza, M. A, L.E. Fernandes, P.P. Silva, R. Ruggiero, E.C. Pereira-Maia, W. Guerra, Complexes of platinum and palladium with 4-nitrobenzoic hydrazide: synthesis and cytotoxic activity, Cent. Eur. J. Chem. 11 (2013) 290, https://doi.org/10.2478/s11532-012-0156-5.
[23] J. do Couto Almeida, I.M. Marzano, F.C.S. De Paula, M. Pivatto, N.P. Lopes, P.C. De Souza, F.R. Pavan, A.L.B. Formiga, E.C. Pereira-Maia, W. Guerra, Complexes of platinum and palladium with β-diketones and DMSO: synthesis, characterization, molecular modeling, and biological studies, J. Mol. Struct. 1075 (2014) 370–376, https://doi.org/10.1016/j.molstruc.2014.07.023.
[24] L.M. Sousa, W.A. Souza, D.A. Paixão, R.B. Fazzi, D.Y. Tezuka, C.D. Lopes, Z.A. Carneiro, M.B. Moreira, M. Pivatto, A.V.G. Netto, S. de Albuquerque, F.B. Ferreira, R.J. De Oliveira, J.A.L.C. Resende, R.C. Lino, R.J. De Oliveira Júnior, A.M. Da Costa Ferreira, W. Guerra, DNA binding, cleavage, apoptosis and cytotoxicity studies of three heteroleptic nickel complexes bearing β-diketones, Inorg. Chim. Acta. 511 (2020) 119824, https://doi.org/10.1016/j.ica.2020.119824.
[25] D.A. Paixão, B.C.A. de Oliveira, J. do Couto Almeida, L.M. Sousa, C.D. Lopes, Z.A. Carneiro, D.Y. Tezuka, J.C.T. Clavijo, J. Ellena, L. Polloni, P.H.A. Machado, S. de Albuquerque, R.J. de Oliveira Júnior, S. Guilardi, W. Guerra, Crystal structure, anti-Trypanosoma cruzi and cytotoxic activities of Cu(II) complexes bearing β-diketone and α-diimine ligands, Inorg. Chim. Acta. 499 (2020) 119164, https://doi.org/10.1016/j.ica.2019.119164.
[26] U. Kalinowska, K. Matławska, L. Chęcińska, M. Domagała, R. Kontek, R. Osiecka, J. Ochocki, Synthesis, spectroscopy and antiproliferative activity of cis- and trans-platinum(II) complexes with diethyl (pyridin-4-ylmethyl)phosphate. X-ray crystal structure of trans-Pt(II) complex, J. Inorg. Biochem. 99 (2005) 2024–2031, https://doi.org/10.1016/j.jinorgbio.2005.06.030.
[27] D. Nieto, A.M. Gonzalez-Vadillo, S. Bruna, C.J. Pastor, C. Ríos-Luci, L.G. Leon, J.M. Padrón, C. Navarro-Ranningera, I. Cuadrado, Heterometallic platinum(II) compounds with β-aminoethylferrocenes: synthesis, electrochemical behaviour and anticancer activity, Dalton Trans. 41 (2012) 432–441, https://doi.org/10.1039/C1DT11358E.
[28] L.P. de Oliveira, Í.P. de Souza, D.A. Paixão, L.M. Sousa, M.F. Lima, C. de S. Pereira, H. Silva, E.C. Pereira-Maia, W. Guerra, Pt(II) complexes of the type *trans*-[$PtCl_2$(DMSO) (hydrazide)] and *cis*-[$PtCl_2$(hydrazide)$_2$]: solvolysis and cytotoxic activity, J. Mol. Struct. 1192 (2019) 76–81, https://doi.org/10.1016/j.molstruc.2019.04.134.
[29] F.P. Fanizzi, F.P. Intini, L. Maresca, G. Natile, G. Uccello-Barretta, Solvolysis of platinum complexes with substituted ethylenediamines in dimethyl sulfoxide, Inorg. Chem. 29 (1990) 29–33. https://doi-org.ez34.periodicos.capes.gov.br/10.1021/ic00326a007.
[30] N. Aztopal, D. Karakas, B. Cevatemre, F. Ari, C. Icsel, M.G. Daidone, E. Ulukaya, A *trans*-platinum(II) complex induces apoptosis in cancer stem cells of breast cancer, Bioorg. Med. Chem. 25 (2017) 269–276, https://doi.org/10.1016/j.bmc.2016.10.032.
[31] A. Ghezzi, M. Aceto, C. Cassino, E. Gabano, D. Osella, Uptake of antitumor platinum(II)-complexes by cancer cells, assayed by inductively coupled plasma mass spectrometry (ICP-MS), J. Inorg. Biochem. 98 (2004) 73–78, https://doi.org/10.1016/j.jinorgbio.2003.08.014.
[32] S. Łukasiewicz, M. Czeczelewski, A. Forma, J. Baj, R. Sitarz, A. Stanisławek, Breast cancer—epidemiology, risk factors, classification, prognostic markers, and current treatment strategies— an updated review, Cancers 13 (2021) 4287, https://doi.org/10.3390/cancers13174287.

[33] H. Mastalarz, M. Agnieszka, J. Wietrzyk, M. Milczarek, A. Kochel, A. Regiec, Synthesis of platinum(II) complexes with some 1-methylnitropyrazoles and in vitro research on their cytotoxic activity, Pharmaceuticals 13 (2020) 433, https://doi.org/10.3390/ph13120433.
[34] M.P. Dhaduk, R.A. Dabhi, V. D Bhatt, B.S. Bhatt, M.N. Patel, Synthesis, characterization, biomolecular interaction, cytotoxicity, and computational studies of quinoxaline-based platinum(II) complexes, Results in Chemistry 7 (2024) 101265, https://doi.org/10.1016/j.rechem.2023.101265.
[35] Z. Momenimovahed, H. Salehiniya, Epidemiological characteristics of and risk factors for breast cancer in the world, Breast Cancer 11 (2019) 151–164.
[36] M. Vojtek, M.P.M. Marques, I. Ferreira, H. Mota-Filipe, C. Diniz, Anticancer activity of palladium-based complexes against triple-negative breast cancer, Drug Discov. Today 24 (2019) 1044–1058.
[37] A.S. Levenson, V.C. Jordan, MCF-7: the first hormone-responsive breast cancer cell line, Cancer Res. 57 (1997) 3071–3078. http://www.ncbi.nlm.nih.gov/pubmed/9242427.
[38] M. Dean, T. Fojo, S. Bates, Tumour stem cells and drug resistance, Nat. Rev. Cancer 5 (2005) 275–284.
[39] A. Bergamo, P.J. Dyson, G. Sava, The mechanism of tumour cell death by metal-based anticancer drugs is not only a matter of DNA interactions, Coord. Chem. Rev. 360 (2018) 17–33.
[40] M. Sirajuddin, S. Ali, A. Badshah, Drug-DNA interactions and their study by UV-Visible, fluorescence spectroscopies and cyclic voltametry, J. Photochem. Photobiol. B Biol. 124 (2013) 1–19.
[41] S.U. Rehman, T. Sarwar, M.A. Husain, H.M. Ishqi, M. Tabish, Studying non-covalent drug-DNA interactions, Arch. Biochem. Biophys. 576 (2015) 49–60.
[42] A. Rodger, B. Nordén, Circular Dichroism and Linear Dichroism, Oxford University Press, Oxford, 1997.
[43] A. Kellett, Z. Molphy, C. Slator, V. McKee, N.P. Farrell, Molecular methods for assessment of non-covalent metallodrug-DNA interactions, Chem. Soc. Rev. 48 (2019) 971–988.
[44] J. Ruiz, C. Vicente, C. de Haro, D. Bautista, Novel bis-C,N-cyclometalated iridium(III) thiosemicarbazide antitumor complexes: interactions with human serum albumin and DNA, and inhibition of cathepsin B, Inorg. Chem. 52 (2013) 974–982.
[45] J.C. Peberdy, J. Malina, S. Khalid, M.J. Hannon, A. Rodger, J. Inorg. Biochem. 101 (2007) 1937–1945.
[46] A. Cano, M. Pérez-Moreno, I. Rodrigo, et al., The transcription factor Snail controls epithelial–mesenchymal transitions by repressing E-cadherin expression, Nat. Cell Biol. 2 (2000) 76–83, https://doi.org/10.1038/35000025.